Ab initio pseudopotential calculations of the atomic and electronic structure of the Ta (100) and (110) surfaces

Christine J. Wu, L. H. Yang, John E. Klepeis, and C. Mailhiot
Lawrence Livermore National Laboratory, University of California, Livermore, California 94551
(Received 20 March 1995)

We have performed *ab initio* pseudopotential plane-wave calculations of both the atomic and electronic structure of the Ta (100) and (110) surfaces. The atomic relaxation of Ta (110) is calculated while our results for the structure of Ta (100) agree well with previous experimental reports. We find that the topmost interlayer separations contract relative to their bulk values by (12±1)% and (2±1)% for Ta (100) and (110), respectively. The changes in the second and deeper interlayer separations differ in sign. The calculated surface formation and relaxation energies are 1.92 eV/atom and −0.17 eV/atom for the relaxed Ta (100) surface and 1.18 eV/atom and −0.03 eV/atom for the relaxed (110) surface. We have also calculated the work functions for both surfaces and find values of 4.0±0.1 eV for (100) and 4.9±0.1 eV for (110), which are both in good agreement with experiment. Our study of the respective surface states and their variation as a function of the relaxation indicates that, in contradiction to a previous report, the surface states do not provide the driving force for the relaxations. We report our calculation of the [110] zone boundary phonon frequencies for bulk Ta. Lastly, this work demonstrates that the pseudopotential method can be applied accurately and efficiently even in the case of a column V transition metal such as Ta.

I. INTRODUCTION

The study of clean Ta surfaces provides a starting point for understanding Ta surface reactions, many of which have important technological applications. For instance, in flat panel liquid crystal display technology the fabrication of self-aligned thin film transistors commonly involves etching and oxidation of Ta thin films. Despite numerous studies there are still a number of open questions regarding the atomic and electronic structure of the Ta (100) and (110) surfaces. Using *ab initio* electronic structure methods we are able to address some of these questions.

Theory can play an important role in the determination of surface structure since in some cases experiments provide only incomplete or approximate structural information. For example, scanning tunneling microscopy (STM) does not yield direct information regarding interlayer relaxation normal to the surface. Iterative multiple-scattering calculations and a proposed structural model are required for low-energy electron diffraction (LEED) analyses. Ion scattering and photoelectron diffraction (PD) also require proposed structures but the accompanying calculations are less complex than those required for LEED. The error bars associated with these experimental determinations depend, among other things, on the sensitivity of the measured data to the structural parameters. This sensitivity can sometimes be quite small for certain structural quantities, leading to big error bars on those quantities. An alternative approach is to obtain the surface geometry from *ab initio* total energy calculations. In recent years, advances in computer technology have made this approach a viable means for accurate structural determinations using density-functional-based methods.

LEED experiments on both the Ta (100) and (110) surfaces have revealed no indications of surface reconstruction[1–5] (lowering of the bulk-terminated 1×1 symmetry) and, therefore, only relaxations involving the expansion or contraction of interlayer separations have been considered in the present as well as earlier studies. The geometry of the Ta (100) surface has been investigated using both LEED and PD techniques with good agreement between the two. A structural study of Ta (100) was carried out by Titov and Moritz[1] using LEED with multiple-scattering calculations in which the first and second interlayer separations were the only adjustable parameters. They found that the topmost Ta (100) interlayer separation contracts relative to its bulk value by (11±2)% while the second interlayer separation expands by (1±2)%. There is a significant (0.75 eV) Ta 4*f* surface core-level shift for the (100) surface which enabled Bartynski *et al.*[6,7] to determine the surface structure using PD. The best match between the data and their multiple-scattering calculations corresponded to a (10±5)% contraction of the topmost interlayer separation, which was their only independent variable. As part of a study[8] of the electronic structure of Ta (100) it was briefly mentioned that a total energy calculation predicted a 13.2% topmost interlayer contraction. However, the calculational details and sublayer relaxations were never published. Our calculated value of (12±1)% for the topmost interlayer contraction is consistent with all of these previous studies. In contrast to Ta (100), the surface structure of Ta (110) has not been studied previously. We find that the contraction of the topmost interlayer separation is only (2±1)% which is small relative to the sensitivity of many experimental techniques.

In the case of covalently bonded materials, such as Si, the energy gain associated with reducing the number of

dangling bonds provides the driving force for many surface relaxations and reconstructions. The surface states associated with these dangling bonds show pronounced energy shifts as a function of the rehybridization or rebonding which differentiates the relaxed or reconstructed surface from the unrelaxed, bulk-terminated surface. The presence of an energy gap in these materials means that these energy shifts are directly correlated with changes in the total energy. In contrast, we expect that the large density of electronic states near the Fermi energy in metals will damp out the effect on the total energy of any shifts in the surface states as a function of the relaxation. Our study of the electronic structure of the Ta (100) and (110) surfaces confirms that there is no simple correlation between shifts in the surface states and the magnitude of the relaxation. This finding is in contradiction to previous reports.[8,9]

The surface electronic structure of Ta (100) has been investigated both experimentally and theoretically; however, to our knowledge there are no first-principles electronic structure calculations for a fully relaxed surface. A theoretical study of a Ta surface was carried out by Feibelman *et al.*[10] using a non-self-consistent local density approximation (LDA) method applied to the (100) surface of hcp rather than bcc Ta. The previous studies of bcc Ta (100) were carried out for comparison to the (100) surfaces of group VIB elements, such as W, which also have bcc crystal structures.[8,11,12] Unlike Ta (100), W (100) undergoes a temperature-dependent reconstruction. Krakauer[11] performed LDA calculations for an unrelaxed five-layer Ta (100) slab and identified surface states that are occupied for W (100) but not for Ta (100) and concluded that this difference is responsible for the fact that W (100) reconstructs but Ta (100) does not. Using inverse photoemission, Bartynski and Gustafsson[12] observed several unoccupied surface states of Ta (100) within 2 eV of the Fermi level, which agreed semiquantitatively with Krakauer's calculations. However, further experiments contradicted the suggestion that the W (100) surface reconstruction is driven by these surface states, since unoccupied surface states were also observed for W (100) and Mo (100).[12] Surface resonances for Ta (100) were observed by Pan *et al.*[8] using angle-resolved photoemission, and confirmed by their LDA calculations for Ta (100) supercells with a 14% contraction of the topmost interlayer separation. They also suggested that enhancement in the bonding character of the $\bar{\Delta}_2$ surface resonances is the driving force for the large interlayer contraction. Using a tight-binding Green function method, Baquero and Coss[9] suggested that the shifts in the surface resonances at the $\bar{\Gamma}$ point, just above the Fermi level, are directly related to the contraction of the topmost Ta (100) interlayer separation.

There have been fewer studies of the Ta (110) surface and they have all focused on an interesting surface-state to surface-resonance transition near the zone center of the surface Brillouin zone. This transition was observed in the photoemission study of Kneedler *et al.*[13,14] In order to understand the transition, van Hoof *et al.*[15] performed electronic structure calculations using a surface-embedded Green function method. In their calculations the substrate is represented by an embedding potential obtained from a bulk calculation.

In this paper we report on the determination of the atomic geometry of Ta (110) using an *ab initio* total energy method. Our calculation of the Ta (100) surface structure gives results which are consistent with previous experimental determinations. We have also evaluated the surface formation and relaxation energies and discuss them in the context of two previously proposed models. These surface energetics play an important role in surface phenomena (e.g., surface properties of alloys, surface growth, and fracture) and have not been reported previously, to our knowledge. In addition, we have calculated the electronic structure of both the relaxed and unrelaxed Ta (100) and (110) surfaces which we compare directly to the bands of bulk bcc Ta, projected onto the respective surface Brillouin zones. Our emphasis is not on the identification of surface states, as in previous studies, but rather on the correlation between surface relaxation and shifts in these surface states. In contradiction with previous reports,[8,9] our study shows that changes in the surface states do not act as the dominant driving force for the Ta surface relaxations and that the Ta surface bonds are delocalized.

II. COMPUTATIONAL DETAILS

A. Surface model

Both the Ta (100) and (110) surfaces were modeled by supercell geometries for which periodic boundary conditions were imposed in all three dimensions. Only interlayer expansion or contraction was considered and therefore both surfaces were assumed to have (1×1) symmetry. We used the theoretical lattice constant[16] of 3.22 Å which corresponded to the volume where the calculated pressure[17] was zero in bulk bcc Ta. In all cases the Ta slabs were separated by vacuum regions with thicknesses greater than 17 Å, which was large enough so that the electrostatic potentials were flat in the middle of the vacuum.

The convergence with respect to slab size was checked by comparing results from seven- and ten-layer calculations for Ta (100). We found that properties determined from the total energy, such as the structure and relative energies, converged quickly with respect to the number of layers. The seven-layer slab was found to be sufficient for the surface geometry and the surface formation and relaxation energies (see Secs. III B and III C). In the case of the electronic structure, we found that ten (100) layers were needed in order to effectively eliminate the artificial splitting of the surface bands which resulted from the weak interaction between the two surfaces of the slab. The interlayer separation for (110) planes was larger than that for (100) planes and therefore a smaller number of (110) planes were needed to achieve convergence. Thus we only considered a seven-layer Ta (110) slab which was similar in thickness to the ten-layer (100) slab.

B. Methods

The present *ab initio* electronic structure calculations were performed within the framework of density functional theory[18] (DFT) and the local density approximation (LDA) for the exchange-correlation functional. We used the Ceperley-Alder[19] exchange-correlation potential as parametrized by Perdew and Zunger.[20] The interaction between the core and valence electrons of Ta was described by a nonlocal and norm-conserving pseudopotential constructed using the scheme of Troullier and Martins.[21] This first-principles Ta pseudopotential was generated from a scalar relativistic all-electron atomic calculation for the spin-polarized Ta ground state configuration $5d^3 6s^2 6p^0$. The $6s$ potential was chosen as the local component with the $5d$ and $6p$ components expressed in the nonlocal separable form of Kleinman and Bylander.[22] The cutoff core radii for $5d$, $6s$, and $6p$ potentials were 1.510, 2.686, and 3.445 bohr, respectively. The Bloch wave functions were expanded in a plane-wave basis set with a kinetic-energy cutoff of 40 Ry, which gave absolute total energy convergence to within 0.01 eV. All of the bulk Ta calculations reported here, including the pressure calculations which determined the theoretical lattice constant, were carried out with this same cutoff.

The **k**-point integrations for the bulk calculations were done using the special **k**-point scheme[23] with a mesh of 8×8×8 points in the Brillouin zone (26 points in the bcc irreducible wedge). For the supercell calculations a smaller mesh of 4×4×2 was used, which corresponds to three and six points in the supercell wedges of Ta (100) and Ta (110), respectively. We found that results for an 8×8×2 mesh (ten points in the wedge) were the same as those obtained with the 4×4×2 mesh for the surface structure of the ten-layer Ta (100) slab, and that the total energy difference was less than 0.05 eV/atom. The Fermi level was determined at each iteration using the Gaussian integration method[24] with a Gaussian broadening of 15 mRy. The conjugate gradient iterative diagonalization scheme was used to obtain the self-consistent solutions of the one-electron Kohn and Sham equations.[25] The forces on the nuclei were evaluated using the Hellmann-Feynman theorem with all atoms allowed to move freely, and the quasi-Newton method[26] was used to find the relaxed atomic positions. We did not include spin-orbit interactions in either the bulk or surface calculations because a previous study[8] showed them to be only a small perturbation on the bulk Ta band structure.

III. RESULTS AND DISCUSSION

A. Transferability of the Ta pseudopotential and Ta bulk phonons

A pseudopotential with good transferability not only can reproduce the all-electron calculation for the atomic configuration in which it was generated, but also has the ability to properly describe the valence-core interaction in different bonding environments. The parameter that directly relates to this transferability is the size of the pseudopotential core radius. In most cases a smaller core leads to better transferability, but also to a deeper potential which requires a larger number of plane waves to achieve convergence in the total energy. In order to test the performance of our Ta pseudopotential in a solid-state environment, we conducted a comparison study of the equilibrium properties of bulk bcc Ta using the pseudopotential plane-wave method and a full potential linear muffin-tin orbital (FP-LMTO) method.[27,28] In both cases we used the same 8×8×8 **k**-point mesh (26 irreducible points) and the Ceperley-Alder[19] exchange-correlation potential.

Figure 1 demonstrates the excellent agreement, especially below the Fermi level, between the bulk bcc band structure of Ta computed using the pseudopotential method (circles) and that obtained with the FP-LMTO method (solid line); most of the circles lie directly on top of the solid line. The ground state properties of bulk bcc Ta (listed in Table I) were obtained by fitting the total energy at nine different volumes using the Murnaghan equation of state.[29] The pseudopotential lattice constant[16] is 2% smaller than the experimental value but only 1% smaller than the FP-LMTO value. The bulk modulus calculated with the pseudopotential method is 9% larger than experiment while the value obtained from the FP-LMTO method is 3% larger than experiment. These differences between the two methods and between each of the methods and experiment are typical for LDA-based calculations. In addition, the overestimates of the bulk moduli relative to experiment are partially due to the fact that the lattice constants are underestimated. The two methods yield similar values for the cohesive energy of bulk Ta; the theoretical values listed in Table I both include a +1.12 eV/atom spin polarization contribution from the Ta free atom, which was calculated with the FP-LMTO method. Even with this spin polarization contribution, both methods significantly over-

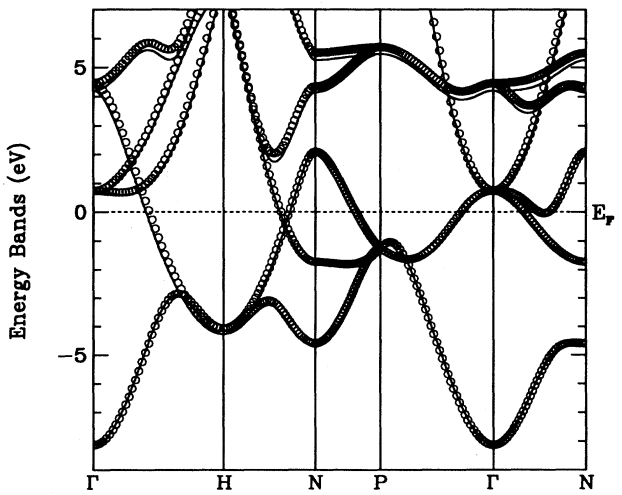

FIG. 1. Comparison of the bulk bcc Ta band structures obtained using an all-electron FP-LMTO method (solid line) and the plane-wave pseudopotential method (circles).

TABLE I. Comparison of the lattice constant (a_0), bulk modulus (B_0), and cohesive energy of bulk bcc Ta obtained with the pseudopotential method to those obtained from all-electron FP-LMTO calculations and from experiment.

	a_0 (Å)	B_0 (Mbar)	E_{coh} (eV/atom)
Pseudopotential	3.23	2.11	9.88
FP-LMTO	3.26	1.98	9.54
Experiment	3.295 ($T = 0$ K)[a]	1.93±0.05[b]	8.10[c]

[a]B. Eisenmann and H. Schäfer, in *Structure Data of Elements and Intermetallic Phases*, edited by K.-H. Hellwege and A. M. Hellwege, Landolt-Börnstein, New Series, Group III, Vol. 14, Pt. a (Springer-Verlag, Berlin, 1988).
[b]A. G. Every and A. K. McCurdy, in *Low Frequency Properties of Dielectric Crystals*, edited by D. F. Nelson, Landolt-Börnstein, New Series, Group III, Vol. 29, Pt. a (Springer-Verlag, Berlin, 1992).
[c]Reference 36.

estimate the cohesive energy compared to experiment, which is also typical for LDA-based calculations. Since the pseudopotential calculations yield results for the Ta bulk properties which are consistent with the all-electron calculations, we conclude that our Ta pseudopotential provides a good representation of the Ta valence-core interaction in a crystalline environment.

We have used this Ta pseudopotential to investigate an interesting experimental observation of the phonons in bulk Ta. In 1964, Wood[30] reported measurements of bulk Ta phonon frequencies using neutron inelastic scattering; he found an accidental degeneracy between the longitudinal and one of the transverse modes (T_2) at the [110] zone boundary. No additional experimental or theoretical studies have been conducted since this original finding. We have calculated the phonon frequencies at the [110] zone boundary using the frozen phonon method and the results are listed in Table II. Our calculation of the longitudinal mode frequency does not match the experimental measurement; our result is 0.37 THz higher than Wood's value of 4.35 THz. However, the two calculated transverse mode frequencies of 4.17 THz (T_2) and 2.74 THz (T_2) agree fairly well with the measured values of 4.35±0.06 THz and 2.63±0.08 THz. The reason for the discrepancy in the case of the longitudinal mode is not known.

B. Surface geometries of Ta (100) and (110)

We have determined the surface atomic structure of Ta (100) from total energy minimizations of seven- and ten-layer supercells and the results are given in Table III. There are small differences between the structures obtained with the two supercells. We have estimated the uncertainty in our interlayer separations to be ±1% due to the flatness of the total energy surfaces. The relaxation of the Ta (100) surface is characterized primarily by a large contraction of the topmost interlayer separation, which was calculated to be (12±1)% with the ten-layer supercell, in excellent agreement with previous reports of (11±2)% and (10±5)%.[1,6,7] As expected, this topmost contraction is accompanied by smaller expansions in the second and third interlayer separations. For example, the second interlayer separation is found to expand by (3±1)% in the ten-layer calculation, somewhat larger than the previous value of (1±2)% obtained by Titov and Moritz[1] from their LEED analysis. Nonetheless, our result falls within the range of their error bars.

The (110) surface is the most close-packed surface for a bcc crystal and therefore we expect it to have a smaller relaxation than the (100) surface. Each (110) surface atom is missing only two nearest neighbors compared to four in the case of a (100) surface atom. Indeed, our seven-layer calculation yields only a (2±1)% contraction of the topmost Ta (110) interlayer separation (see Table IV). This value is similar in magnitude to the experimental uncertainties in previous studies of the (100) surface. A number of 4*d* bcc transition metals exhibit similar trends for (100) and (110) surface relaxations. For example, Methfessel *et al.*[31] carried out FP-LMTO calculations for Nb (100), Nb (110), Mo (100), and Mo (110) and obtained contractions of the topmost interlayer separations of 9.3%, 3.7%, 9.0%, and 3.9%, respectively. For these bcc transition metals the contraction (expansion) of the topmost interlayer for the (100) surface appears to be approximately 2–3 times larger than for the (110) surface.

TABLE II. Comparison of the calculated phonon frequencies (in THz) at the [110] zone boundary with those measured in Ref. 30.

Normal mode	LDA	Experiment
$\bar{1}10$ (L)	4.72	4.35±0.08
$\bar{1}10$ (T_1)	2.74	2.63±0.08
001 (T_2)	4.17	4.35±0.06

TABLE III. Interlayer relaxations (Δd_{ij}) for Ta (100), listed as percentages of the bulk separation (1.61 Å) and obtained from seven- and ten-layer supercell calculations. Negative and positive values refer to interlayer contraction and expansion, respectively.

Interlayer indices (ij)	Δd_{ij} (%) (seven-layer)	Δd_{ij} (%) (ten-layer)
1-2	−12	−12
2-3	4	4
3-4	4	3
4-5		0
5-6		0

TABLE IV. Interlayer relaxations (Δd_{ij}) for Ta (110), listed as percentages of the bulk separation (2.79 Å) and obtained from a seven-layer supercell calculation. Negative and positive values refer to interlayer contraction and expansion, respectively.

Interlayer indices (ij)	Δd_{ij} (%) (seven-layer)
1-2	−2
2-3	3
3-4	3

C. Surface formation and relaxation energies of Ta (100) and (110)

The process of creating a surface may be viewed as consisting approximately of three independent steps: (1) diabatic cleavage of the crystal (frozen electronic charge density), (2) electronic equilibration to the Born-Oppenheimer surface for fixed atom positions (bulk-terminated surface), and (3) self-consistent atomic and electronic relaxation to the global minimum. The surface formation energy σ is the combined total energy cost associated with all three steps. It depends on the surface orientation and is typically proportional to the surface roughness. Values of σ are usually reported either in units of energy per surface atom or per unit surface area. We will use units of energy per surface atom in order to emphasize the connection between σ and chemical bonding. The dominant contribution to σ is often the energy cost to break bonds in step (1), which we call the cleavage energy, $E_{\rm clv}$. The energy associated with step (2), the electronic energy $E_{\rm el}$, reflects the difference between the surface bonds on the unrelaxed surface and the bulk bonds. In the case of semiconductors, which have directional bonding, $E_{\rm el}$ is typically small compared to $E_{\rm clv}$, but we will see shortly that $E_{\rm el}$ is important in the case of Ta. The surface relaxation energy $E_{\rm rlx}$ is the energy gain resulting from the self-consistent atomic and electronic relaxations in step (3). We will estimate $E_{\rm el}$ by using the calculated values of σ and $E_{\rm rlx}$ and an approximation to $E_{\rm clv}$ based on a previously proposed model.

We have calculated σ and $E_{\rm rlx}$ directly from the total energies:

$$\sigma = (E_{\rm slab}^{\rm relaxed} - NE_{\rm bulk})/2$$

and

$$E_{\rm rlx} = (E_{\rm slab}^{\rm relaxed} - E_{\rm slab}^{\rm unrelaxed})/2,$$

where $E_{\rm slab}^{\rm relaxed}$ and $E_{\rm slab}^{\rm unrelaxed}$ are the total energies of N-atom slabs in their relaxed and unrelaxed atomic configurations. $E_{\rm bulk}$ is the total energy per atom of the bulk crystal. The factor of 1/2 accounts for the two surfaces in our supercell model. The calculated values of σ for both surfaces (σ_{100} and σ_{110}) are listed in Table V. We find that the seven- and ten-layer calculations give similar values of σ_{100}, consistent with the small effect of supercell size on the surface geometry (see Sec. III B). Using a seven-layer supercell we calculate $\sigma_{110} = 1.18$ eV/atom which is significantly smaller than the value of $\sigma_{100} = 1.92$ eV/atom. The fact that the (110) surface costs less energy to create than the (100) surface is not unexpected in view of the smaller number of missing nearest neighbors for a (110) surface atom compared to a (100) surface atom. However, the relationship between σ and the number of missing nearest neighbors is not quite linear, as can be seen from the fact that the ratio of σ_{100} to σ_{110} is less than 2. The surface free energy of Ta at its melting temperature was estimated to be 2.49 J/m^2 by Tyson and Miller[32] using liquid surface tension data and 2.27 J/m^2 by Mezey and Giber[33] using the free enthalpy of atomization. Since a liquid minimizes its surface free energy we expect that σ for the more close-packed (110) surface will be closer to the liquid value. In these alternate units we find $\sigma_{110} = 2.58$ J/m^2 which confirms this expectation. We have also found, as in several previous studies of other metals,[34,35] that $E_{\rm rlx}$ is small ($E_{\rm rlx}^{100} = -0.17$ eV/atom; $E_{\rm rlx}^{110} = -0.03$ eV/atom; only 6%–8% of σ for both surfaces). In general, we expect that the inclusion of $E_{\rm rlx}$ in the calculation of σ is not crucial for metals with no surface reconstruction.

TABLE V. Calculated surface formation energies (σ) in units of energy per surface atom and per unit surface area, and the surface relaxation energies ($E_{\rm rlx}$) per surface atom for both Ta (100) and (110) surfaces.

	Ta (100) (seven-layer)	Ta (100) (ten-layer)	Ta (110) (seven-layer)
σ (eV/atom)	1.82	1.92	1.18
σ (J/m^2)	2.82	2.97	2.58
$E_{\rm rlx}$ (eV/atom)	−0.13	−0.17	−0.03

A commonly used expression for σ has a simple linear dependence on the number of missing nearest neighbors and the cohesive energy of the bulk crystal:

$$\sigma = \frac{(C_{\rm bulk} - C_{\rm sur})}{C_{\rm bulk}} E_{\rm coh},$$

where $C_{\rm bulk}$ and $C_{\rm sur}$ are the coordination numbers of a bulk atom and a surface atom, respectively. This expression assumes that the cohesive energy for a bulk atom, $E_{\rm coh}$, can be approximated as a sum of energies which correspond only to the number of nearest-neighbor "bonds." Bonds for surface atoms and bonds for bulk atoms are assumed to have the same bond strength. This "frozen bond-cutting model" considers only the energy associated with step (1) ($\sigma = E_{\rm clv}$), corresponding to a diabatic process with no electronic relaxation. For this reason it serves only as an upper bound to the actual surface formation energy. Typically it gives correct trends as a function of surface roughness and it is a better representation of σ for semiconductors than for metals. With $E_{\rm coh}$ taken from experiment [$E_{\rm coh}^{\rm expt} = 8.10$ eV/atom (Ref. 36)], this model yields 4.05 eV/atom and 2.025 eV/atom for Ta (100) and (110), respectively, which represent estimates of $E_{\rm clv}$. Using these values for $E_{\rm clv}$ and our *ab initio* results for σ and $E_{\rm rlx}$, we estimate $E_{\rm el} = \sigma - E_{\rm rlx} - E_{\rm clv}$ to be −1.96 eV/atom and −0.81 eV/atom for Ta (100) and (110), respectively. $E_{\rm el}$ re-

flects the difference between the surface and bulk bond strengths and is apparently a significant contribution to σ in the case of Ta.

The effect of electronic relaxation on the surface energy [step (2)] can be approximately taken into account by treating the nearest-neighbor bond strength in the "square-root bond-cutting model."[31] In this model

$$\sigma = \frac{(\sqrt{C_{\rm bulk}} - \sqrt{C_{\rm sur}})}{\sqrt{C_{\rm bulk}}} E_{\rm coh},$$

which is obtained from an approximation to tight-binding theory. Methfessel *et al.*[31] have shown, using FP-LMTO calculations, that this equation works well for the 4*d* transition metals. In contrast, the pseudopotential calculations of Wright *et al.*[34] indicate that this model underestimates σ by nearly 30% for the (100) surface of the simple metal Mg. In the case of the 5*d* transition metal Ta ($E_{\rm coh}^{\rm expt} = 8.10$ eV/atom (Ref. 36)], this equation gives $\sigma_{100} = 2.37$ eV/atom and $\sigma_{110} = 1.09$ eV/atom, in fairly good agreement with our *ab initio* results of $\sigma_{100} = 1.92$ eV/atom and $\sigma_{110} = 1.18$ eV/atom. For the 4*d* transition metal Nb, the element one row above Ta in the Periodic Table, Methfessel *et al.*[31] calculated $\sigma_{100} = 1.86$ eV/atom and $\sigma_{110} = 1.08$ eV/atom. In the context of the bond-cutting models, the larger surface formation energies of Ta relative to Nb are consistent with the fact that Ta has a bigger cohesive energy than Nb.

D. Work functions and charge transfer for Ta (100) and (110)

The planar averaged valence electron charge densities for the relaxed (dashed line) and unrelaxed (solid line) seven-layer Ta (100) slabs (ρ_e^{100}) are plotted in Fig. 2 as a function of the z coordinate normal to the (100) surface. The z coordinates of the Ta atoms in the relaxed and unrelaxed supercells are indicated by the empty and solid circles, respectively. We note that ρ_e^{100} peaks in between adjacent Ta (100) layers, which corresponds to the midpoint of the nearest-neighbor bonds where we expect the valence electron charge density to be largest. In the case of the (100) planes there are no in-plane nearest-neighbor pairs, but there are four in-plane nearest-neighbor pairs per atom among the atoms in a given (110) plane. Therefore the planar averaged valence electron charge density for Ta (110) (ρ_e^{110} in Fig. 3) peaks at the z coordinates of the Ta layers instead. For both surfaces, relaxed and unrelaxed, we have found that the electronic charge transferred from the bulk to the surface layer is small (less than $0.1e$); the total valence electronic charge integrated from the middle of the vacuum to the middle of the first interlayer is close to $5e$ (the valence electronic charge for an isolated Ta atom). For the unrelaxed slabs, the small enhancement in the peak values of ρ_e^{100} and ρ_e^{110} in the topmost layers represents the charge rearrangement due to the formation of the surface. For the relaxed (100) surface, the large increase in the peak value of ρ_e^{100} near the surface is primarily due to the 12% decrease of the interlayer separation rather than any significant bulk-to-surface charge transfer.

The work functions for the Ta (100) and (110) surfaces, calculated for both the relaxed and unrelaxed geometries, are listed in Table VI. The error bars associated with the numerical integration procedure required to obtain the work functions are estimated to be ± 0.1 eV. The absolute differences between the seven- and ten-layer Ta

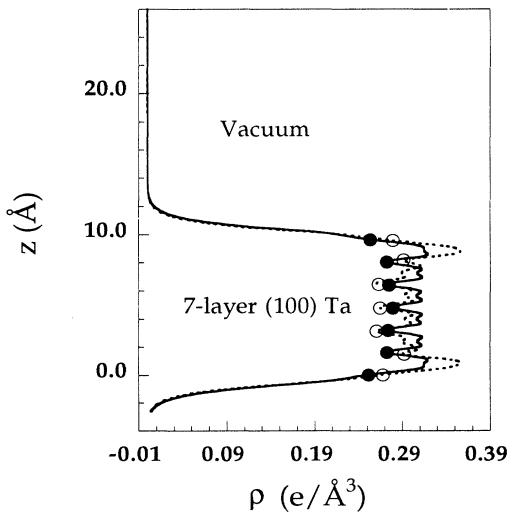

FIG. 2. Calculated planar averaged valence electron charge density (ρ) as a function of the z coordinate normal to the [100] direction for the relaxed (dashed line) and unrelaxed (solid line) seven-layer Ta (100) slab. The empty and solid circles indicate the z coordinates of the Ta atoms and ρ at these coordinates for the relaxed and unrelaxed slabs, respectively.

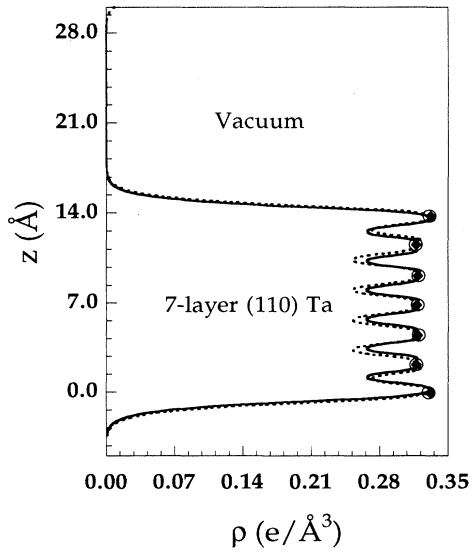

FIG. 3. Calculated planar averaged valence electron charge density (ρ) as a function of the z coordinate normal to the [110] direction for the relaxed (dashed line) and unrelaxed (solid line) seven-layer Ta (110) slab. The empty circles and solid diamonds indicate the z coordinates of the Ta atoms and ρ at these coordinates for the relaxed and unrelaxed slabs, respectively.

TABLE VI. Work functions (eV) calculated for the relaxed and unrelaxed Ta (100) and (110) surfaces. The error bars for the calculated work functions were estimated to be ±0.1 eV.

	Ta (100)			Ta (110)	
	(seven-layer)	(ten-layer)	experiment	(seven-layer)	experiment
Relaxed	3.8	4.0	4.15[a]	4.9	4.80[a]
Unrelaxed	4.1	4.3		4.9	

[a]Reference 37.

(100) calculations are of this same order of magnitude while the differences between the work functions of the relaxed and unrelaxed surfaces appear to be even better converged. The relaxed ten-layer (100) slab yields a work function of 4.0±0.1 eV, which agrees well with the experimental value of 4.15 eV.[37] The change in work function due to relaxation is small for Ta (100), on the order of −0.3 eV, and nearly indistinguishable for Ta (110), due to the much smaller interlayer contraction for Ta (110). The seven-layer Ta (110) slab has a similar thickness as the ten-layer Ta (100) and was used to calculate the work function for the (110) surface. It gives a work function of 4.9±0.1 eV, in excellent agreement with the experimental value of 4.8 eV.[37]

E. Effects of surface relaxation on the surface electronic structure

In order to study the correlation between the surface electronic structure and surface relaxation, we have calculated the band structures for both the fully relaxed and the bulk-terminated surfaces. The energy bands of the unrelaxed and relaxed ten-layer Ta (100) slabs are plotted as the solid dots and lines, respectively, in Fig. 4. The gray area corresponds to the bulk bcc Ta continuum projected onto the (100) surface Brillouin zone. The supercell bands are shifted so that the average electrostatic potential in the most bulklike layers is equal to the corresponding potential in the true bulk. We note that the Fermi level E_F is effectively constant as a function of the surface relaxation, which is consistent with the fact that for metals the dominant contribution to the density of electronic states near E_F comes from the bulk bands. Figure 4 also indicates that the (100) surface of bcc Ta is rich in surface states independent of the surface relaxation.

We find that the multilayer (100) relaxations cause small, but noticeable shifts (less than ±0.3 eV) in the bands throughout the energy spectrum, including the bulklike bands. It is interesting to note that these shifts are of the same order of magnitude as the corresponding shift in the work function (see Table VI). In a supercell calculation, where the semi-infinite bulk is approximated by a finite number of layers, even the bulklike states sample the surface region significantly. For this reason, a change in the surface potential can shift not only the positions of surface bands but also those of the bulklike bands. We do not find any simple correspondence between the sign of the relaxation-induced energy shifts and the position of the surface states relative to E_F; the shifts are of both signs for states above and below E_F. In Fig. 4 there is a gap in the bulk projected bands approximately 1 eV below E_F along the direction $\bar{X} \rightarrow \bar{M}$. We note that the state which overlaps the bulk continuum (surface resonance) just above this gap for the unrelaxed (100) surface drops inside the gap when the surface is allowed to relax. Obviously, this surface state contributes to the surface relaxation. However, all of the surface states shift and none of them were found to drop in energy by substantially more than the average energy shift. This result merely reflects the many-body nature of the delocalized bonding at metal surfaces.

There have been two previous studies which investigated the correlation between the Ta (100) surface relaxation and the surface states. Weinert and co-workers[8] calculated the band structure for the unrelaxed Ta (100) surface and for a (100) surface with a 14% contraction in the topmost interlayer separation, using a linearized augmented-Slater-type-orbital method. They suggested that shifts in the $\bar{\Delta}_2$ (along $\bar{\Gamma} \rightarrow \bar{X}$) surface resonances were the driving force for the surface relaxation. Later, by comparing the tight-binding band structure of the unrelaxed surface and a surface with a 13.5% contraction in the topmost interlayer separation, Baquero and Coss[9] concluded that the surface resonances at the $\bar{\Gamma}$ point was directly linked to the large interlayer contraction. In our calculations we do find that the positions of all these surface resonances change upon relaxation, but not by a

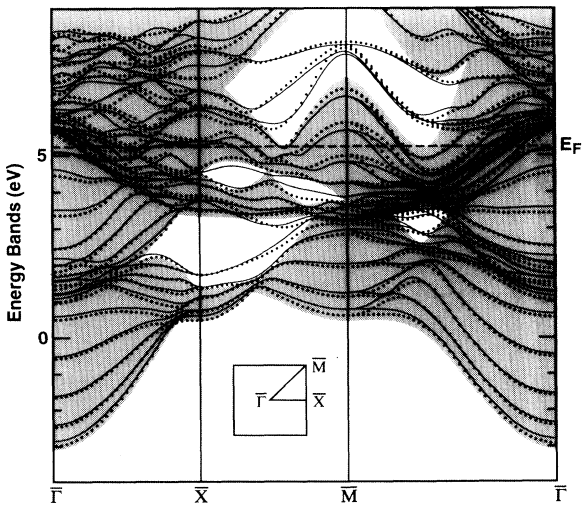

FIG. 4. Energy bands of the unrelaxed (dots) and relaxed (lines) ten-layer Ta (100) slabs. The gray area represents the bulk bcc Ta continuum projected onto the (100) surface Brillouin zone.

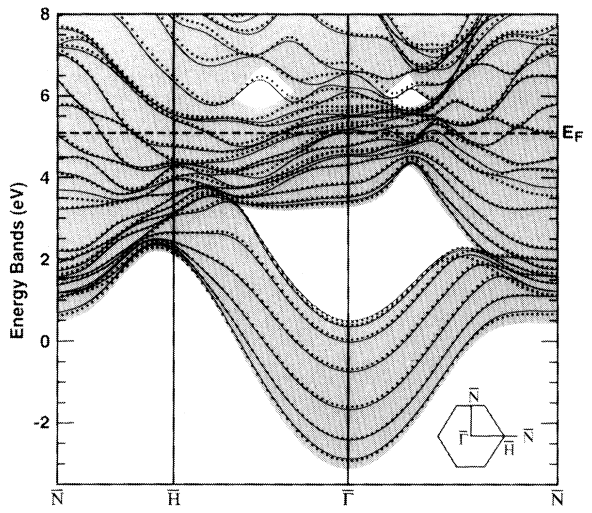

FIG. 5. Energy bands of the unrelaxed (dots) and relaxed (lines) seven-layer Ta (110) slabs. The gray area represents the bulk bcc Ta continuum projected onto the (110) surface Brillouin zone.

significant amount compared to the average shift. Therefore we believe that no particular surface state acts as the driving force for the Ta (100) surface relaxation.

The band structure of Ta (110) responds to the surface relaxation in a manner similar to that of Ta (100). The energy bands obtained from the unrelaxed and relaxed seven-layer Ta (110) slabs are plotted as the solid dots and lines, respectively, in Fig. 5. Once again, the supercell bands are shifted in order to align the bulk electrostatic potentials. The gray area corresponds to the bulk bcc Ta continuum projected onto the (110) surface Brillouin zone. We note that our projected bands differ significantly from the tight-binding results used by Kneedler *et al.*[13,14] and van Hoof *et al.*[15] For instance, in contrast to the tight-binding result, our bulk projected bands show no gap approximately 1–3 eV below E_F along the direction $\bar{N} \rightarrow \bar{H}$. In addition, the two tight-binding calculations give quite different gap structures approximately 0–2 eV above the E_F. As in the case of Ta (100), both the Ta (110) surface and bulklike bands shift in response to the surface relaxation. The average change in the band energies is smaller for Ta (110) than for Ta (100), consistent with the smaller relaxation. As for the (100) surface, no evidence for a surface-state-driven relaxation is found for Ta (110).

IV. SUMMARY

We have generated a nonlocal and norm-conserving Ta pseudopotential and tested its transferability in a solid-state environment against an all-electron FP-LMTO method. Comparison of the calculated ground state properties and band structure of bulk bcc Ta demonstrates the excellent agreement between the two methods. The validity of this pseudopotential enabled us to perform a detailed study on the Ta (100) and (110) surface structures as well as the correlation between surface relaxation and the surface electronic structure, using the pseudopotential plane-wave method. We obtained a large (12±1)% contraction of the topmost interlayer separation for Ta (100), which agrees very well with previous experimental reports.[1,6,7] We have performed calculations of the Ta (110) surface relaxations and predict that the contraction of the topmost interlayer separation is (2±1)%. In contrast to the conclusions of previous studies, we found no simple correlation between the surface states and the surface relaxation. We also report calculated values for the surface formation and relaxation energies as well as the work functions of the Ta (100) and (110) surfaces. Finally, we have presented our calculations of the [110] zone boundary bulk bcc Ta phonon frequencies.

ACKNOWLEDGMENTS

This work was performed under the auspices of the U.S. Department of Energy by the Lawrence Livermore National Laboratory under Contract No. W-7405-ENG-48. We would like to thank Jannette Bradley and Danial A. Fletcher for their assistance in producing the plots of the projected band structures.

[1] A. V. Titov and W. Moritz, Surf. Sci. **123**, L709 (1982).
[2] S. T. Ceyer, A. J. Melmed, J. J. Carroll, and W. R. Graham, Surf. Sci. **144**, L444 (1984).
[3] Z. T. Stott and H. P. Hughes, Vacuum **31**, 487 (1981).
[4] W. K. Kuhn, R. A. Campbell, and D. W. Goodman, J. Phys. Chem. **97**, 446 (1993).
[5] L. A. DeLouise, Surf. Sci. **324**, 233 (1995).
[6] R. A. Bartynski, D. Heskett, K. Garrison, G. Watson, D. M. Zehner, W. N. Mei, S. Y. Tong, and X. Pan, J. Vac. Sci. Technol. A **7**, 1931 (1989).
[7] R. A. Bartynski, D. Heskett, K. Garrison, G. M. Watson, D. M. Zehner, W. N. Mei, S. Y. Tong, and X. Pan, Phys. Rev. B **40**, 5340 (1989).
[8] X. Pan, E. W. Plummer, and M. Weinert, Phys. Rev. B **42**, 5025 (1990).
[9] R. Baquero and R. D. Coss, Phys. Status Solidi **169**, K69 (1992).
[10] P. J. Feibelman, J. A. Appelbaum, and D. R. Hamann, Phys. Rev. B **20**, 1433 (1979).
[11] H. Krakauer, Phys. Rev. B **30**, 6834 (1984).
[12] R. A. Bartynski and T. Gustafsson, Phys. Rev. B **35**, 939 (1987), and references therein.
[13] E. Kneedler, D. Skelton, and S. D. Kevan, Phys. Rev. Lett. **64**, 315 (1990).
[14] E. Kneedler, K. E. Smith, D. Skelton, and S. D. Kevan, Phys. Rev. B **44**, 8233 (1991).
[15] J. B. A. N. van Hoof, S. Crampin, and J. E. Inglesfield, J. Phys. Condens. Matter **4**, 8477 (1992).
[16] The lattice constant determined from the pressure calculations is slightly different than the value obtained from the

equation of state (see Sec. III A). In order to avoid spurious nonzero pressure, we used the lattice constant obtained from the pressure calculations in the determinations of the surface structures. This choice is consistent with the usage of the Hellmann-Feynman forces in the energy minimizations.

[17] O. H. Nielsen and R. M. Martin, Phys. Rev. B **32**, 3780, 1985.

[18] P. Hohenberg and W. Kohn, Phys. Rev. **136**, B864 (1964).

[19] D. M. Ceperley and B. J. Alder, Phys. Rev. Lett. **45**, 566 (1980).

[20] J. P. Perdew and A. Zunger, Phys. Rev. B **23**, 5048 (1981).

[21] N. Troullier and J. L. Martins, Phys. Rev. B **43**, 1993 (1991).

[22] L. Kleinman and D. M. Bylander, Phys. Rev. Lett. **48**, 1425 (1982).

[23] H. J. Monkhorst and J. D. Pack, Phys. Rev. B **13**, 5188 (1976).

[24] C. L. Fu and K. M. Ho, Phys. Rev. B **28**, 5480 (1983).

[25] W. Kohn and L. J. Sham, Phys. Rev. **140**, A1133 (1965).

[26] W. H. Press, S. A. Teukolsky, W. T. Vetterling, and B. P. Flannery, *Numerical Recipes in Fortran*, 2nd ed. (Cambridge, New York, 1992), p. 418.

[27] M. Methfessel, Phys. Rev. B **38**, 1537 (1988).

[28] M. Methfessel, C. O. Rodriguez, and O. K. Andersen, Phys. Rev. B **40**, 2009 (1989).

[29] F. D. Murnaghan, Proc. Natl. Acad. Sci. U.S.A. **30**, 244 (1944).

[30] A. D. B. Woods, Phys. Rev. **136**, A781 (1964).

[31] M. Methfessel, D. Hennig, and M. Scheffler, Phys. Rev. B **46**, 4816 (1992).

[32] W. R. Tyson and W. A. Miller, Surf. Sci. **62**, 267 (1977).

[33] L. Z. Mezey and J. Giber, Jpn. J. Appl. Phys. **21**, 1569 (1982).

[34] A. F. Wright, P. J. Feibelman, and S. R. Atlas, Surf. Sci. **302**, 215 (1993).

[35] M. Yamamoto, C. T. Chan, and K. M. Ho, Phys. Rev. B **50**, 7932 (1994).

[36] C. Kittel, *Introduction to Solid State Physics,* 5th ed. (John Wiley & Sons, New York, 1976), p. 74.

[37] H. B. Michaelson, J. Appl. Phys. **48**, 4729 (1977).

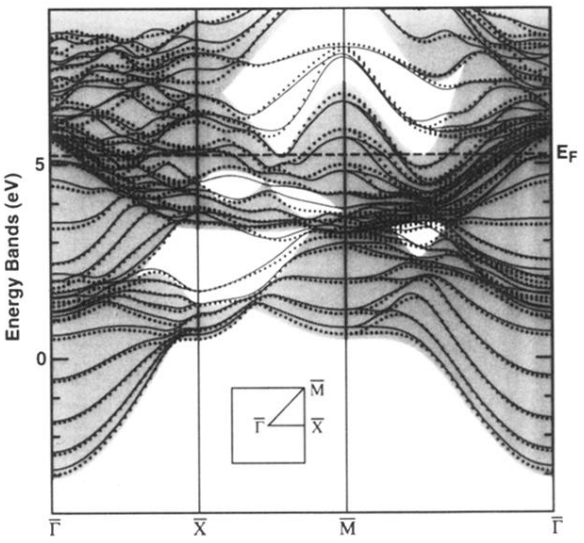

FIG. 4. Energy bands of the unrelaxed (dots) and relaxed (lines) ten-layer Ta (100) slabs. The gray area represents the bulk bcc Ta continuum projected onto the (100) surface Brillouin zone.

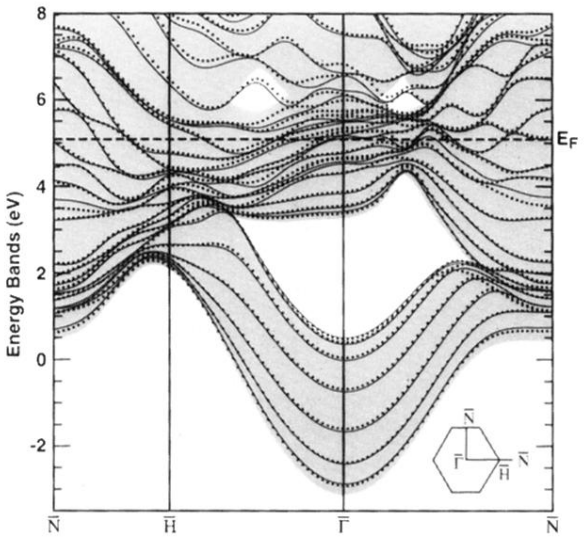

FIG. 5. Energy bands of the unrelaxed (dots) and relaxed (lines) seven-layer Ta (110) slabs. The gray area represents the bulk bcc Ta continuum projected onto the (110) surface Brillouin zone.